2017

Embryonic Development of the Annual Killifish Austrofundulus limnaeus: An Emerging Model for Ecological and Evolutionary Developmental Biology Research and Instruction

Jason E. Podrabsky
Portland State University, podrabsj@pdx.edu

Claire L. Riggs
Portland State University, rclaire@pdx.edu

Amie L. Romney
Portland State University, arom2@pdx.edu

S. Cody Woll
Portland State University, scwoll@pdx.edu

Josiah T. Wagner
Portland State University

Citation Details

Podrabsky, J. E., Riggs, C. L., Romney, A. L., Woll, S. C., Wagner, J. T., Culpepper, K. M., & Cleaver, T. G. (2017). Embryonic development of the annual killifish Austrofundulus limnaeus: An emerging model for ecological and evolutionary developmental biology research and instruction. Developmental Dynamics.

DEVELOPMENTAL DYNAMICS 246:779–801, 2017 THE AUTHORS DEVELOPMENTAL DYNAMICS PUBLISHED BY
DOI: 10.1002/DVDY.24513

RESEARCH ARTICLE

Embryonic Development of the Annual Killifish *Austrofundulus limnaeus*: An Emerging Model for Ecological and Evolutionary Developmental Biology Research and Instruction

Jason E. Podrabsky,* Claire L. Riggs, Amie L. Romney, S. Cody Woll, Josiah T. Wagner, Kristin M. Culpepper, and Timothy G. Cleaver

Department of Biology, Portland State University, Portland, Oregon

Background: ***Austrofundulus limnaeus*** **is an annual killifish from the Maracaibo basin of Venezuela. Annual killifishes are unique among vertebrates in their ability to enter into a state of dormancy at up to three distinct developmental stages termed diapause I, II, and III. These embryos are tolerant of a wide variety of environmental stresses and develop relatively slowly compared with nonannual fishes. Results: These traits make them an excellent model for research on interactions between the genome and the environment during development, and an excellent choice for developmental biology laboratories. Furthermore, *A. limnaeus* is relatively easy to maintain in a laboratory setting and has a high fecundity, making it an excellent candidate as an emerging model for studies of development, and for defining the limits of developmental buffering in vertebrates. Conclusions: This study reports for the first time on the detailed development of *A. limnaeus* and provides a photographic and illustrated atlas of embryos on the two developmental trajectories possible in this species. *Developmental Dynamics 246:779–801, 2017*. © 2017 The Authors Developmental Dynamics published by Wiley Periodicals, Inc. on behalf of American Association of Anatomists**

Key words: diapause; embryo; development; emerging model organism; mid-blastula transition

Submitted 8 March 2017; First Decision 18 April 2017; Accepted 18 April 2017; Published online 8 May 2017

Introduction

Development in the annual killifishes is unique for several reasons that makes them excellent models for studies of ecological and evolutionary developmental biology. First, the embryos are able to enter into diapause, a reversible state of metabolic depression, at up to three distinct stages of development (Wourms, 1972a, 1972c). Second, there are at least two distinct developmental trajectories associated with entry into diapause along which the embryos can develop, depending on both maternal and environmental cues (Podrabsky et al., 2010; Furness et al., 2015). Third, the process of epiboly and gastrulation or axis formation are spatially and temporally separated by a distinct dispersion and subsequent reaggregation of the embryonic (deep) blastomeres (Wourms, 1972b). These developmental stages are only present in annual killifishes, and evidence suggests they can act as a developmental buffer against cell damage or loss during extended durations in diapause I, which can occur during these stages (Wourms, 1972c; Wagner and Podrabsky, 2015). Fourth, they grow incredibly fast to sexual maturity, and some species are able to complete their entire adult lifespan from hatching to senescence and death in a matter of weeks, making them a powerful emerging model for studies on vertebrate aging (Genade et al., 2005). Fifth, their tolerance of environmental stresses such as extremes in oxygen availability is unparalleled in the world of vertebrate embryos (Podrabsky et al., 2016). Finally, diapause and the "annual" life history that includes all of the traits listed above is thought to have evolved independently in Africa and South America, and possibly multiple times in South America alone (Furness et al., 2015; Furness, 2016). The unique biology of annual killifishes makes them attractive emerging models for development that can offer insights into aspects of biology not possible with traditional model organisms.

Development of annual killifishes was first described in detail for *Austrofundulus myersi* (Dahl, 1958), by John Wourms, and most studies use Wourms' stages to describe developmental progression (Wourms, 1972a,b,c). While this work was critical for describing the general developmental pattern of annual killifishes, *A. myersi* was never widely available to the scientific community and a detailed photographic atlas of the developmental

Grant sponsor: The National Science Foundation; Grant number: IOS-1354549.
*Correspondence to: Jason E. Podrabsky, Department of Biology, Portland State University, Portland, OR 97201. E-mail: jpod@pdx.edu

Article is online at: http://onlinelibrary.wiley.com/doi/10.1002/dvdy.24513/abstract

stages was not provided. In 1995, *Austrofundulus limnaeus* (Schultz, 1949) an annual killifish from the Maracaibo Basin of Venezuela, was collected specifically for use as a scientific model of development in annual killifishes and the study of diapause (Podrabsky et al., 1998; Podrabsky, 1999). These fish survive in some of the most extreme conditions possible, even for annual killifishes (Polačik and Podrabsky, 2015; Podrabsky et al., 2016). Their savanna and coastal desert habitats offer a mix of relatively predictable and unpredictable environmental cues and factors that have led to a highly robust developmental program that appears to be infused with the potential to generate variation. In addition to their extremophile biology, these fish are relatively easy to maintain in captivity, highly fecund, and share many of the characteristics of traditional model organisms. Recent work on this species has resulted in the availability of an annotated draft genome (Wagner et al., 2015), and a wealth of transcriptomic data to detail the expression of genes across development and in response to environmental stresses (Romney et al., 2015), and to identify those transcripts that are maternally packaged (Romney and Podrabsky, 2017).

Here, we describe the embryonic development of *A. limnaeus* at 25°C using Wourms' stages as a guide. This work is not meant to replace Wourms' staging but rather to augment and update this work, and to provide specifics for development of *A. limnaeus*, which differs in many subtle and yet important aspects of its development from *A. myersi*. We hope that others will adopt *A. limnaeus* as a model for studies of developmental biology, and use this fascinating fish in biology teaching labs as a way to encourage future generations of developmental biologists to leverage what we have learned in traditional model organisms to explore the incredible diversity in development that is critical for the generation and maintenance of biodiversity, and the colonization and exploitation of unique and interesting ecological niches.

Results and Discussion

Developmental Stages

The descriptions below are not an all-inclusive atlas of features, but rather are meant to orient the viewer and highlight the major features of each developmental stage. A more detailed list of features organized by physiological systems is provided for late stage embryos in Table 1. Also, illustrations of some of the key developmental stages and an illustration to the key features of these embryos are provided in Figure 10.

Stage 1. *Unfertilized egg (Figs.* 1*A*, 10*A*). The egg is oval in shape. The egg envelope (chorion) is covered with fine, sticky, hair-like projections. A clear micropyle funnel is apparent at one end of the elongated axis of the egg. No perivitelline space is present, and the yolk appears "cloudy" due to the presence of cortical granules under the vitelline membrane. Many lipid droplets of various sizes are present in the yolk. These droplets move freely if the egg is rotated.

Stage 2. *Fertilized egg (Fig.* 1*B).* The perivitelline space has formed between the egg envelope and the vitelline membrane. The yolk clears as the cortical granules fuse with the vitelline membrane. Cytoplasmic filaments can be seen under the site of fertilization and material can be observed moving toward the animal pole.

Stage 3. *One-cell stage (Figs.* 1*C*, 10*B*). A single large blastomere has formed at the animal pole. Materials from the yolk are still moving into the forming blastomere.

Stage 4. *Two-cell stage (Figs.* 1*D*, 10*C*). There are two blastomeres of roughly equal size as a result of the first meroblastic cleavage.

Stage 5. *Four-cell stage (Figs.* 1*E*, 10*D*). The second cleavage results in four blastomeres of roughly equal size.

Stage 6. *Eight-cell stage (Figs.* 1*F*, 10*E*). The third cleavage results in eight cells of roughly equal size that are arranged in a circular shape.

Stage 7. *Sixteen-cell stage (Figs.* 1*G*, 10*F*). Some blastomeres are completely surrounded by other blastomeres as the cells form a solid mass.

Stage 8. *Thirty-two-cell stage (Figs.* 1*H*, 10*G*). Cell division and rearrangement form a solid blastoderm with an outer layer of cells that completely invest a handful of inner cells that are rounded in appearance. Cells in the outer layer begin to flatten and expand laterally while also forming close attachments to each other which gives the blastoderm a smooth outer surface.

Stage 9. *Sixty-four-cell stage (Figs.* 1*I*, 10*H*). Blastomere number is difficult to track, and cleavage synchrony is lost. The outer layer of blastomeres continues to flatten.

Stage 10. *High solid blastula (Figs.* 1*J*, 10*I*). There are over 100 cells, but cell counting is difficult. The blastoderm is a solid mass of cells with two clear populations, the outer layer of flattening cells and the inner mass of circular cells.

Stage 11. *Flat solid blastula (Figs.* 1*K*, 10*J*). Cell number is similar to the previous stage. The solid blastula of cells starts to flatten in shape as the outer layer of cells continue to flatten and expand toward the yolk syncytial layer (YSL) at the periphery of the blastoderm.

Stage 12. *Early flat hollow blastula (Figs.* 1*L*, 10*K*). The cells of the outer layer, the enveloping cell layer (ENVL), begin to assume a polygon morphology and have formed a roof that covers an inner segmentation cavity that contains a central mass of round blastomeres. The blastoderm continues to flatten as the outer margins extend outward.

Stage 13. *Late flat hollow blastula (Fig.* 1*M*). The ENVL continues to thin and extend outward toward the periphery of the blastoderm as the cells change shape to become polygons that are very closely opposed. The cells at the periphery of the central mass of circular blastomeres begin to move outward. YSL nuclei at the peripheral boundaries of the blastoderm are visible.

Stage 14. *Expanding flat hollow blastula (Figs.* 1*N*, 10*L*). The central mass of deep cells begins to break up as amoeboid blastomeres migrate toward the periphery of the blastoderm. The enveloping cell layer continues to flatten and expand outward. Several rows of YSL nuclei are now visible.

Stage 15. *Early epiboly (Fig.* 1*O*). Many ameboid blastomeres from the central mass are now migrating toward the periphery of the blastoderm as the enveloping cell layer begins to migrate toward the vegetal pole. Migrating blastomeres may be in contact with the enveloping cell layer, the YSL, or both.

Stage 16. *One-fourth epiboly (Figs.* 1*P*, 10*M*). Approximately one quarter of the yolk surface is now covered by the expanding blastoderm. Many migrating deep blastomeres are found in the peripheral parts of the blastoderm.

Stage 17. *One-half epiboly (Figs.* 2*A*, 10*N*). Half of the yolk surface is covered by the three layers of migrating cells: the ENVL (top), the ameboid blastomeres (middle), and the YSL (bottom). Ameboid blastomere density is still greatest at the animal pole, but most cells are actively migrating.

TABLE 1. Detailed Description of Features in Late Stage Embryos of *Austrofundulus limnaeus*

Stage	Body size	Central nervous system	Sensory systems	Circulatory system	Digestive system, visceral organs	Musculoskeletal system	Pigmentation	Tail and fins
29a	~ 0.7 mm - approximately half the diameter of the yolk.	Neural keel is visible.				3 pairs of somites have formed on either side of the neural keel.		
29b	~ 0.7 mm.					5-6 pairs of somites have formed.		
30a	~0.9 mm.	Neural tube with narrow lumen.	Optic lobes and otic placodes are present.			10 pairs of somites have formed.		
30b	~0.9 mm.	Beginning of brain folding at midbrain-hindbrain interface.	Optic cups and otic vesicles formed. Olfactory placodes condensing.	A straight heart tube has formed and begins to beat. A few small vessels have formed on the yolk surface anterior to the embryo.		14-15 pairs of somites have formed.		
31	~1.4 mm - approximately the diameter of the yolk mass.	Brain fold between midbrain and hindbrain is prominent.	Lens placodes formed and attached to ectoderm, olfactory placodes are visible.	The heart is contracting regularly at approximately 25-30 beats/min. Several vessels are visible on the yolk surface. Clear cells can be seen within vessels or in blood islands on the yolk.		25 pairs of somites have formed.		

TABLE 1. *Continued*

Stage	Body size	Central nervous system	Sensory systems	Circulatory system	Digestive system, visceral organs	Musculoskeletal system	Pigmentation	Tail and fins
32			Lens placodes are still attached to the surface ectoderm.	Heart rate is reduced to approximately 10-15 beats/min. The number and diameter of the blood vessels continue to increase. A clear network of vessels covers the yolk and establishes a complete circuit for circulation of blood. A few clear cells may be observed in circulation, or moving back and forth in response to the contraction of the heart.		38 pairs of somites have formed.		
33			Lens placodes separate from the surface ectoderm, but higher magnification is sometimes needed to see this.	Heart rate declines to less than 10 beats/min in most embryos. Previously circulating blood cells often accumulate in the vasculature, especially where vessels merge.		38-42 pairs of somites have formed.		

TABLE 1. *Continued*

Stage	Body size	Central nervous system	Sensory systems	Circulatory system	Digestive system, visceral organs	Musculoskeletal system	Pigmentation	Tail and fins
34		Expansion of the hindbrain and thinning of hindbrain roof is apparent.	Lens placodes separate from the surface ectoderm and are easily observed. Loosely arranged chondrocytes are present in the otic vesicles.	Heart rate increases to greater than 20 beats/min and the blood cells resume circulation.		38-42 pairs of somites. The most anterior pairs are difficult to see as the head develops. Somite pairs in the anterior third of the embryo being to morph into a chevron shape from a round ball of cells.		
35a	Embryo length is just under half of the circumference of the yolk.		White otoliths are present in the otic vesicles.		A very faint, straight gut tube is barely visible.		A few scattered melanocytes are present on the dorsal aspect of the head.	
35b	Embryo length is just under half of the circumference of the yolk.		Otic vesicles protrude laterally.	Contraction of the heart is a long wave that runs the length of the heart tube. Blood is slightly red due to expression of hemoglobin.	The straight gut accumulates a white substance. The liver forms as a small cluster of cells on the left side of the embryo.			Pectoral fin buds are barely visible posterior to the otic vesicles.
36	Embryo length is approximately half the circumference of the yolk.		Black pigmentation is present at the top of the eyes on the dorsal aspect.	Heart looping starts. Circulating blood cells are now distinctly red in color. The ventricle is apparent as a thickening of the heart tube wall.	The middle portion of the gut tube begins to grow out toward the yolk. The liver grows larger.	There are still only 38-42 pairs of somites. Counting somites becomes very difficult at this stage. Most if not all of the somites have taken a chevron shape. Chondrocytes start to condense into the bodies of the vertebrae.	Many melanocytes cover the anterior two-thirds of the embryo and a few scattered white iridocytes are on the dorsal aspect of the head.	Pectoral fin buds present.
37a								

TABLE 1. *Continued*

Stage	Body size	Central nervous system	Sensory systems	Circulatory system	Digestive system, visceral organs	Musculoskeletal system	Pigmentation	Tail and fins
	Embryo length is just over half the circumference of the yolk.				The gut tube begins the process of looping. The first spots of dark pigmentation are visible on the dorsal surface of the visceral cavity.		Melanocytes are sparsely distributed across nearly the entire dorsal surface of the embryo.	The tail bud begins to lift off the yolk.
37b	Embryo length is approximately two thirds the circumference of the yolk.		The eyes are darkly pigmented. The choroid fissure is visible.	There are now two clear contractile areas of the heart with the future atrium contracting before the future ventricle.	One complete loop of the gut tube is present.		Many melanocytes are present across the dorsal surface extending to the tail. More white iridocytes are forming on dorsal surface of the head.	
38	Embryo length is greater than two-thirds, but less than three quarters the circumference of the yolk.		Reflective material is apparent on the dorsal surface of the eye.	The ventricle walls begin to thicken.	The posterior of the midgut region begins to enlarge. The gall bladder is visible as a green or yellow ball. The dorsal surface of the visceral cavity is quite dark with pigmentation.			
39	Embryo length is three quarters the circumference of the yolk.		Eyes are mottled golden and reflective across the entire surface.		The anterior mid portion of the gut tube begins to enlarge. The lower jaw has formed but is not free. The gall bladder is bright green.	Cartilaginous vertebral bodies are visible with alcian blue staining, but are still diffuse and difficult to count.	Melanocytes and iridocytes cover the head and extend the enire length of the embryo.	Pectoral fin buds are beginning to grow fin tissue toward the posterior of the embryo. The tail bud is raised off the yolk and is starting to flatten and widen as the caudal fin forms.

TABLE 1. *Continued*

Stage	Body size	Central nervous system	Sensory systems	Circulatory system	Digestive system, visceral organs	Musculoskeletal system	Pigmentation	Tail and fins
40	Embryo length is equal to the circumference of the yolk.		A distinct ring of golden and reflective material is present around the lens.	The ventricle walls are distinctly thicker than the atrial walls. Trabeculae are forming on the inner walls of the ventricle. The atrium is to the left and only slightly anterior to the ventricle. The bulbous cordis is easily observed as blood flows out of the heart.	The gut tube continues to enlarge and accumulate a white substance. The oral membrane is open and the embryo can gape. The swimbladder is pigmented.	30-32 cartilaginous vertebrae have formed. The neural and hemal arches form during this stage. Some vertebral bodies begin to ossify late in this stage. The cartilaginous lower jaw apparatus is formed. A cartilaginous capsule begins to form around the otic vesicle. Hypural plate cartilages of the caudal fin are formed.	Many melanocytes and iridocytes. The head is covered and melanocytes start to aggregate in areas.	Pectoral fin buds are easily observed and form a paddle with no rays. The caudal fin has formed and some rays have started to form. Dorsal and anal fin folds are present.
41	Embryo length is greater than the circumference of the yolk and the tip of the tail extends to the rear of the eye.					The vertebral bodies and bases of the arches continue to ossify.	Melanocytes are more densely packed on the head but are scattered across most of the embryo. Iridocytes on the head and upper portion of the trunk begin to turn a brown-orange color.	

TABLE 1. *Continued*

Stage	Body size	Central nervous system	Sensory systems	Circulatory system	Digestive system, visceral organs	Musculoskeletal system	Pigmentation	Tail and fins
42	The tail extends to the back of the head.				The foregut is enlarged. The dorsal surface of the visceral cavity continues to darken with pigment cells.		Iridocytes are now distinctly brown-orange in color on the head and over the anterior two-thirds of the body.	Rays are prominent on the caudal and pectoral fins. No melanocytes are present on the dorsal or anal fin folds, or on the pectoral fins.
43	The tail extends to the back of the head.					There are 30-32 ossified vertebrae with ossified arches. A cartilaginous capsule has formed around the otic vesicles and attaches this portion of the skull to the cartilaginous lower jaw.	Melanocyte density and size continues to increase giving the embryo a distinctly darker appearance than previous stages.	Rays have formed on the portions of the anal and caudal fin folds that will remain as mature fins.
45							Melanocyte and iridocyte density increases, especially in the trunk and tail regions. The body is now distinctly brown in color with black spots.	Melanocytes are present on the dorsal, anal, and pectoral fins. The regions of the dorsal and anal fin folds between the fins and the caudal fin are beginning to regress.

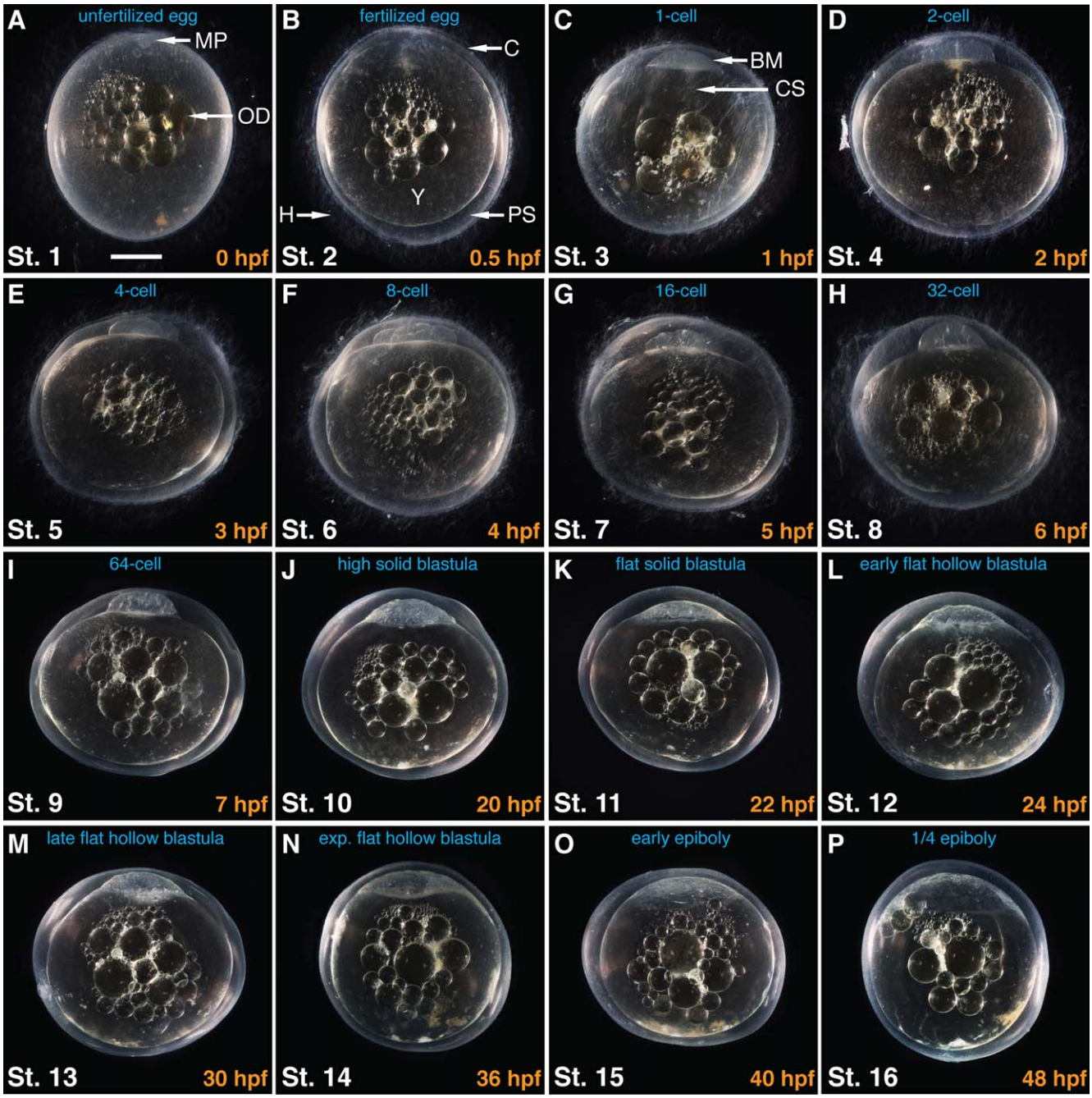

Fig. 1. **A–P:** Fertilization, cleavage, blastula formation, and early epiboly. All images are side views with the animal pole facing up, and the vegetal pole facing down. The descriptive name of the stage is listed in blue at the top of each panel. The stage number is provided in white in the lower left corner. The timing of development at 25°C, in hours postfertilization (hpf) is provided in the lower right hand corner in orange. Note that these times are not exact, but should only be used as an approximation of when these stages typically occur. The hairy projections have been mechanically removed from embryos in panels I–P. The scale bar in the lower portion of panel A indicates a length of 0.5 mm. MP, micropyle; OD, oil droplet; PS, perivitelline space; H, hairy projections; C, chorion; BM, blastomere; CS, cytoplasmic streaming; Y, yolk.

Stage 18. *Three-quarters epiboly (Figs. 2B, 10O).* Three-quarters of the yolk surface is covered and most if not all ameboid cells are actively migrating and relatively evenly distributed across the yolk surface. The smaller lipid droplets in the yolk start to merge and coalesce with other droplets leading to a reduction in the total number of lipid droplets and a larger average size.

Stage 19. *Completion of epiboly (Figs. 2C, 10P).* The yolk mass is now completely invested by the three layers of cells. The ameboid blastomeres are relatively evenly distributed across the yolk and continue to migrate. Ameboid blastomere size is large and the cells are easily observed under a dissecting microscope. The lipid droplets in the yolk continue to coalesce into larger droplets.

Stage 20. *Dispersed phase 1 (Figs. 2D, 3A, 10Q).* The ameboid blastomeres remain large, are more or less randomly distributed across the yolk, and are rarely seen touching other cells. The lipid droplets have coalesced into a single lipid droplet that becomes fixed in place in close apposition to the yolk membrane. Diapause I may occur here if the embryos are left in the presence of adult fish.

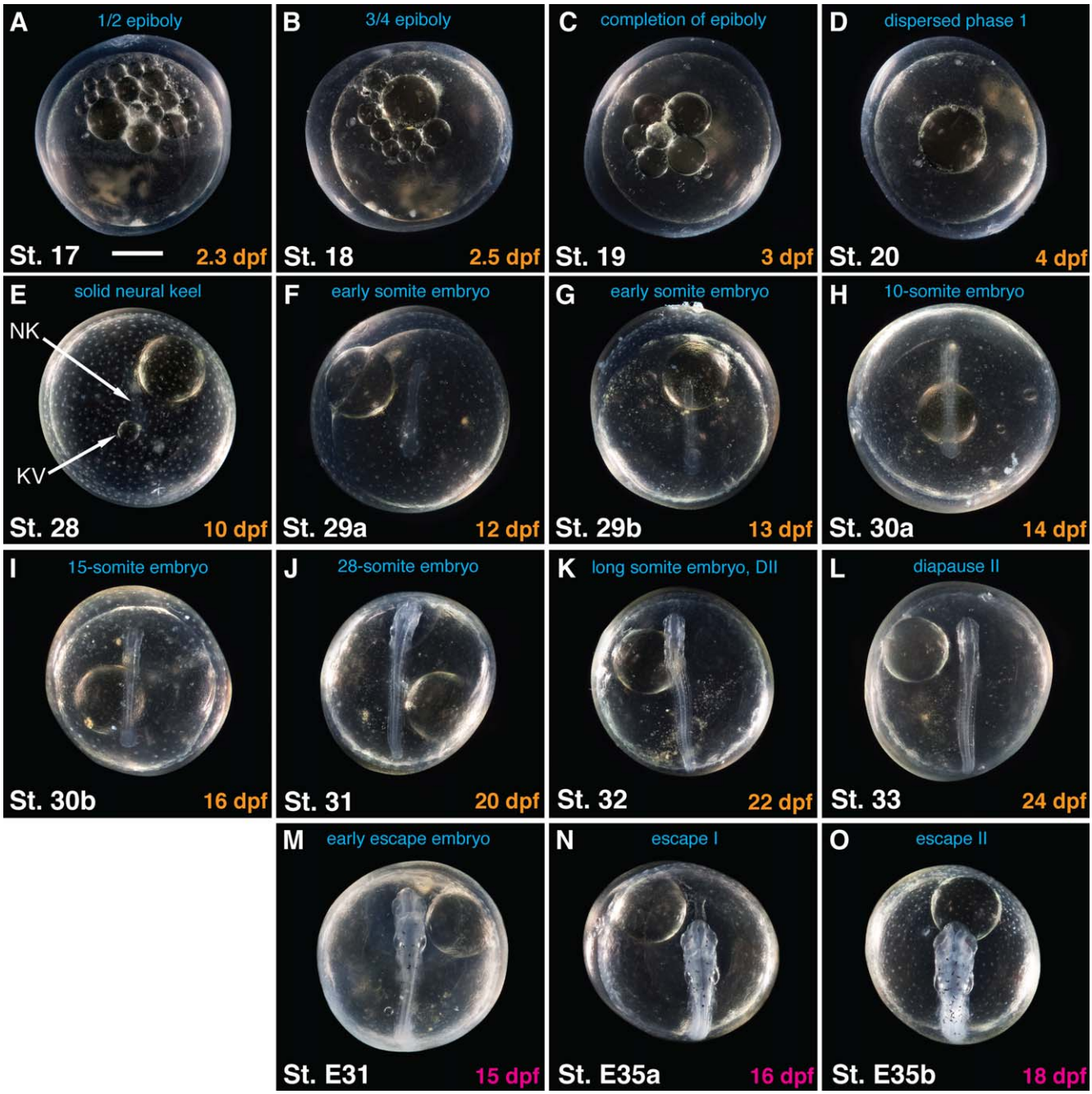

Fig. 2. Late epiboly, dispersion/reaggregation, neurulation, and somitogenesis. **A-D:** Side views with the animal pole facing up. **E–O:** Dorsal views of the embryos with the anterior end facing up. The descriptive name of the stage is listed in blue at the top of each panel. The stage number is provided in white in the lower left corner. The timing of development at 25°C, in days postfertilization (dpf) is provided in the lower right hand corner in orange for embryos on the diapause II trajectory and pink for embryos on the escape trajectory. Note that these times are not exact, but should only be used as an approximation of when these stages typically occur. The scale bar in the lower portion of panel A indicates a length of 0.5 mm. NK, neural keel; KV, Kupffer's vesicle.

Stage 21. *Dispersed phase 2 (Fig. 3B)*. Ameboid blastomere size has decreased to a point that they are difficult to identify through a dissecting microscope. A large group of blastomeres begins to accumulate. The position of the nascent cell aggregate is typically somewhere on the opposite side of the embryo from the lipid droplet and thus is easiest to see when viewed with an inverted microscope.

Stage 22. *Reaggregation 1 (Fig. 3C)*. The aggregate is a monolayer of cells that continues to grow in cell number and density. The area of the aggregate is large and may cover an area equivalent to the original blastoderm or greater.

Stage 23. *Reaggregation 2 (Fig. 4D)*. The aggregate is many layers thick in the middle and only a single layer of cells at the periphery. A distinct accumulation of cells is apparent at one end of the aggregate; this accumulation of cells marks the future posterior end of the embryonic axis.

Stage 24. *Reaggregation 3 (Fig. 4E)*. The aggregate has formed a disc with a pronounced aggregation of cells at the future

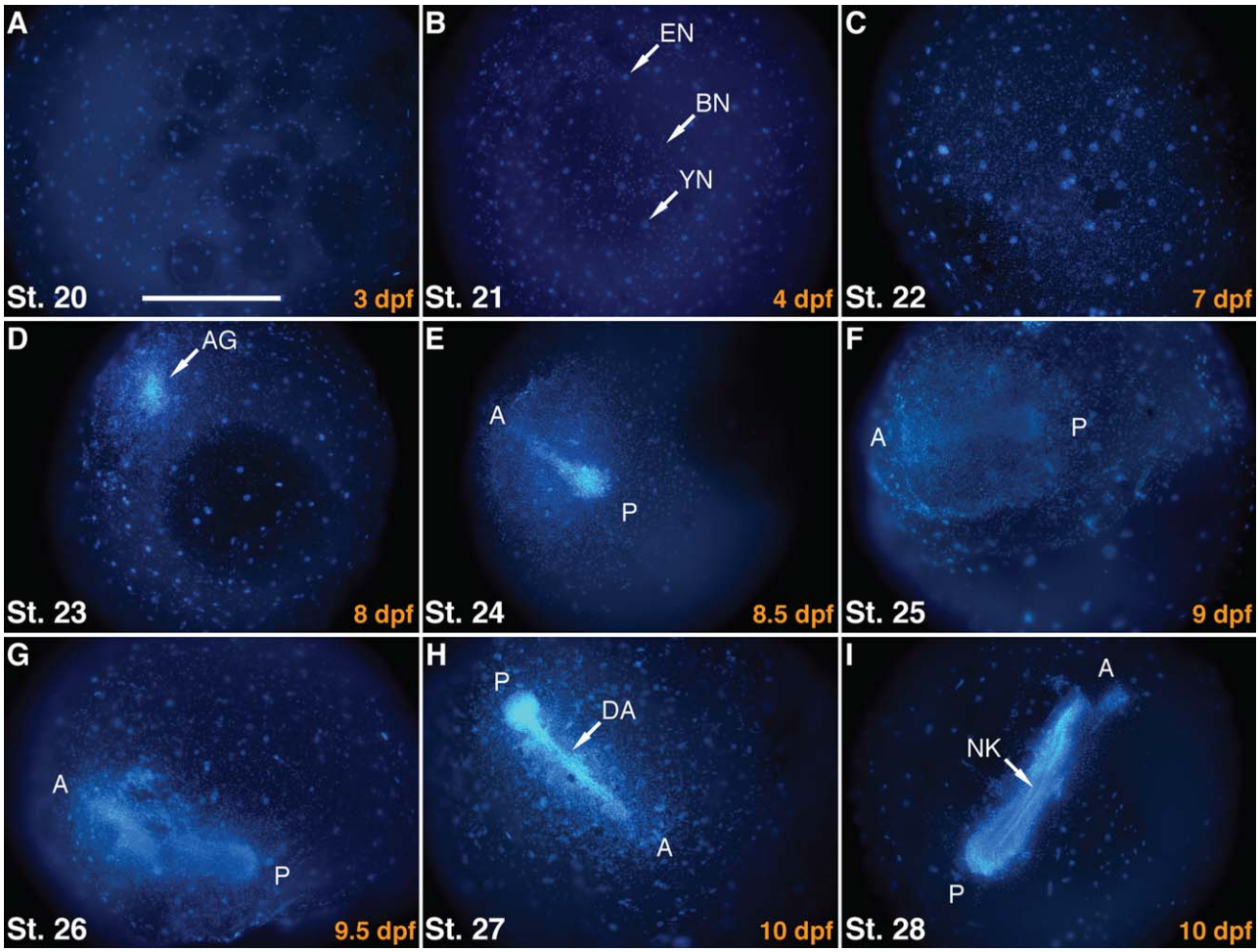

Fig. 3. **A–I:** Dispersion and reaggregation. Hoechst staining of cell nuclei during the dispersion and reaggregation stages of development in fixed and dechorionated embryos. These stages are not easily visible in live specimens. Stage is listed in white in the bottom left corner. The timing of development at 25°C, in days postfertilization (dpf) is provided in the lower right hand corner in orange. Larger nuclei are present in the enveloping cell layer and the yolk syncytial layer although in these images it is difficult to tell the two populations apart. The deep blastomeres typically have small compact nuclei. The scale bar in the lower portion of panel A indicates a length of 0.5 mm. EN, nucleus of an enveloping cell layer cell; BN, nuclei of deep blastomeres; YN, nucleus of the yolk syncytial layer; A, future anterior end of embryo; P, future posterior end of embryo; AG, aggregate; DA, definitive embryonic axis; NK, solid neural keel.

posterior end that now extends toward the anterior of the aggregate. The margins of the aggregate are still a monolayer of cells.

Stage 25. *Reaggregation 4 (Fig.* 3*F*). The aggregate continues to grow in cell number and density and assumes a more oval or elongated shape. The margins of the aggregate are often more than one cell layer thick. Cells continue to accumulate along the midline of the aggregate causing the middle mass to grow in a posterior to anterior pattern.

Stage 26. *Reaggregation 5 (Fig.* 3*G*). Cells continue to accumulate along the midline of the aggregate which causes the overall shape of the aggregate to become more elongate.

Stage 27. *Definitive axis (Fig* 3*H*). Most of the cells have accumulated along the midline of the now elongated aggregate. The embryonic axis is now defined by a forming neural keel with a large round accumulation of cells at the posterior end of the axis. The aggregate is many cell layers thick except at the extreme margins.

Stage 28. *Solid neural keel (Figs.* 2*E*, 3*I*, 10*R*). A solid elongated mass of cells is now visible in living tissue as the neural keel forms and extends approximately half the diameter of the yolk mass (0.7 mm). At the anterior end, a head fold begins to form while at the posterior end a small sphere thought to be similar to Kupffer's vesicle is prominent directly underneath the developing neural keel. At this point, the ENVL begins to lose its attachment to the yolk syncytial layer and many "pillar-like" attachments between these two layers can be seen. This process continues as embryos develop toward diapause II and eventually most of the "pillars" disappear.

Stage 29a. *Early somite embryo (Figs.* 2*F*, 10*S*). The first few pairs of somites form lateral to the neural keel and just anterior to Kupffer's vesicle. The lateral plate mesoderm is apparent on both sides of the embryo as a thin streak. The posterior end of the neural keel is somewhat enlarged and paddle shaped. Separation of the ENVL from the yolk syncytial layer continues and in some embryos a distinct space can be easily seen between the two layers.

Stage 29b. *Early somite embryo (Figs.* 2*G*, 10*T*). The number of somite pairs has increased to five to six. The anterior-most region of the solid neural keel assumes a more triangular shape and just posterior to this two bugles begin to appear on either side of the

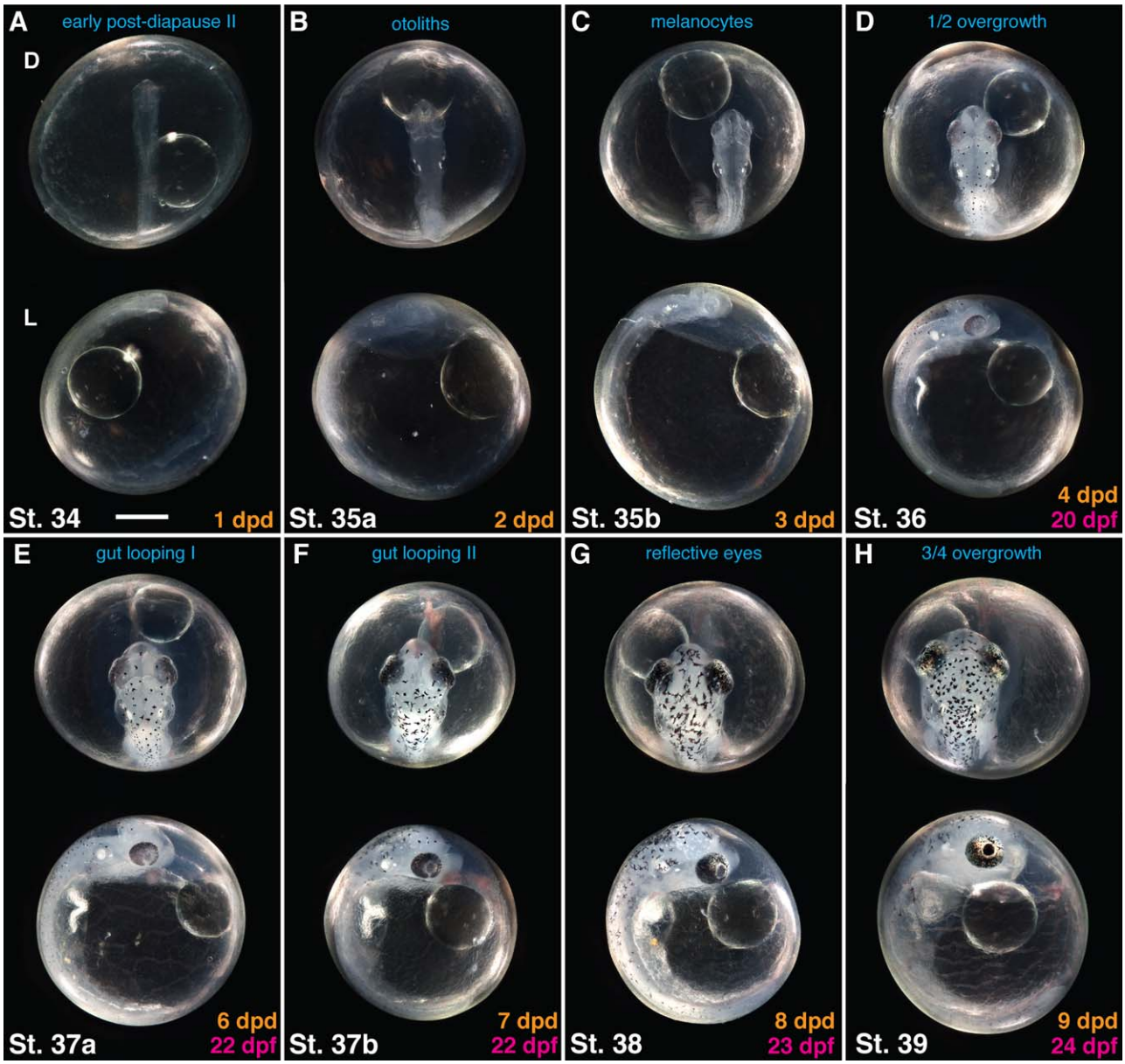

Fig. 4. **A–H:** Organogenesis. Each panel contains a dorsal view of the embryo (D) at the top and a lateral view of the embryo (L) on the bottom. The timing of development at 25°C, in days postdiapause II (dpd) is provided in the lower right hand corner in orange for embryos on the diapause II trajectory and pink for embryos on the escape trajectory in days postfertilization (dpf). Note that these times are not exact, but should only be used as an approximation of when these stages typically occur. The scale bar in the lower portion of panel A indicates a length of 0.5 mm.

neural keel. A clear region of mesoderm is visible anterior to the neural keel.

Stage 30a. *Ten somite embryo (Figs. 2H, 10U).* There are 10 pairs of somites. The narrow lumen of the neural tube is visible. The anterior end of the neural tube has begun to differentiate into clear subregions of the future brain. The optic lobes are formed and small lateral folds of the neural tube begin to form just posterior to them. The otic placodes are visible on the lateral sides of the forming embryo just anterior to the first somite. In some embryos a small cavity can been seen forming inside the placodes. The cardiac plate mesoderm, anterior to the head, has started to fold but no sub-cephalic pocket is visible. Kupffer's vesicle is still visible toward the posterior end of the embryo but is reduced in size.

Stage 30b. *First heart beat (Figs. 2I, 10V).* There are 14–15 pairs of somites. The otic vesicles are visible. Folds in the neural tube continue to develop with a prominent fold forming to mark the division between the mid-brain and hindbrain regions. The lumen of the neural tube is still very narrow. The head has lifted off the yolk and a clear sub-cephalic pocket is now visible. At this stage, the tubular heart located ventral to the developing head region begins to contract. Contractions are irregular at first but quickly establish a rhythm of 10–15 beats/min. Kupffer's vesicle is no longer visible in most embryos.

Stage 31. *Twenty-five somite embryo (Figs. 2J, 10W).* There are 25–28 pairs of somites. The sub-cephalic pocket is now prominent and extends posterior to the regions adjacent to the first pairs of somites. The forming heart tube can be seen anterior to

and ventral to the head region. The heart is beating at 25–30 beats/min, the peak rate in prediapause II embryos. The lumen of the neural tube has expanded in the region of the hindbrain and the rhombomeres in this region are often visible. The otic vesicles are prominent. The optic cups have formed and the lens placodes are beginning to thicken in the overlaying ectoderm. The olfactory placodes are easily identified just medial and anterior to the optic cups.

Stage 32. *Long somite embryo (Figs. 2K, 10X).* There are 38 pairs of somites. The brain region looks more or less the same as in the previous stage. The heart is beating at 10–15 beats/min and vasculature associated with the heart is beginning to form. Blood islands can be seen on the surface of the yolk around the embryo. In some embryos, a few immature red blood cells (clear in color) can be seen circulating or moving back and forth in rhythm with the heart beat as if tethered in place. In some cases a complete vascular circuit is established with a few immature red blood cells circulating.

Stage 33. *Diapause II (Fig. 2L).* There are 38–42 pairs of somites present. The anterior end of the embryo has not changed appreciably since stage 31. The heart is still beating but the rate is decreased to $\leq$ 10 beats/min. In some cases, the heart beat appears to cease. Previously circulating blood cells adhere to the vasculature in various areas (especially where vessels branch or merge) and no longer circulate even if the heart is beating.

Stage E31. *Early escape embryo (Fig. 2M).* This is the earliest stage of the escape trajectory that is observably different from the diapause II trajectory. There are 26–28 pairs of somites. The head is wider and longer than a diapause-bound embryo. A few melanocytes are present on the dorsal aspect of the head region. The expanding folds of the midbrain extend over the optic cups. Loose groups of chondrocytes within the otic vesicles mark the future locations of the otoliths. There are circulating blood cells and the heart rate is greater than 20 beats/min.

Stage E35a. *Escape I (Fig. 2N).* This stage looks essentially like the diapause trajectory stage 35a (Fig. 4B), except that the melanocytes are present on the dorsal aspect of the head region. There are 28–32 pairs of somites.

Stage E35b. *Escape II (Fig. 2O).* This stage looks very similar to diapause trajectory stage 35b, except that black pigment is forming on the dorsal and medial surface of the optic cups. There are 32–38 pairs of somites. In later stages of development, it is not easily possible to tell diapause trajectory and escape trajectory embryos apart.

Stage 34. *Early postdiapause II (Figs. 4A, 10Y).* Diapause II has been terminated or "broken" and the embryo has begun to actively develop again. The embryo extends in length to approximately one-third the circumference of the yolk mass. At first, developmental progress is slow and the first signs of release from diapause II are an increased heart rate ($>$ 20 beats/min) and the circulation of premature red blood cells in the vasculature. The width of the head increases.

Stage 35a. *Otoliths (Fig. 4B).* The embryo has grown in length to cover just under half the circumference of the yolk mass. Two white otoliths are visible within each otic vesicle. The head continues to grow wider as the brain folds increase and brain size/volume continues to increase. The lenses are easily observed within the optic cups.

Stage 35b. *Melanocytes (Fig. 4C).* Brain growth and morphogenesis continue. The otic vesicles are prominent and protrude out from the side of the developing brain. A few scattered melanocytes are visible on the dorsal surface of the hindbrain region. In many embryos, a white material begins to accumulate in the thin, straight gut tube making it easily visible through a dissecting microscope for the first time.

Stage 36. *One-half overgrowth (Figs. 4D, 6A, 10Z).* The embryo now covers approximately half of the circumference of the yolk sphere. Melanocytes sparsely cover the anterior two-thirds of the dorsal surface of the embryo, and a few white iridocytes are visible in the head region. Dark pigmentation in the eyes is visible, starting in the dorsal and medial regions of the optic cup and extending outward as embryos progress through this stage. The brain regions continue to grow and differentiate. The roof of the hindbrain is very thin and the lumen has widened substantially. The gut tube is very white and begins this stage as a straight tube, but by the end has started to develop a slight kink. The pectoral fin buds are easily visible just posterior to the otic vesicles. The anterior somites begin to take on a chevron shape and chondrocytes begin to form the bodies of the vertebrae.

Stage 37a. *Gut looping I (Fig. 4E).* The embryo covers over half the circumference of the yolk mass. The transparency of the lateral roof of the hindbrain is reduced. Melanocytes are visible across almost the entire dorsal surface of the embryo. The gut tube begins to loop. The tail bud is beginning to lift off the yolk.

Stage 37b. *Gut looping II (Fig. 4F).* The embryo covers approximately two-thirds the circumference of the yolk mass. The transparent nature of the hindbrain roof is now greatly diminished giving the whole head region a more "white" coloration. The eyes are very darkly pigmented, and the choroid fissure is clearly visible. The number of melanocytes and iridocytes continue to increase. Looping of the white gut tube is complete.

Stage 38. *Reflective eyes (Figs. 4G, 10A′).* The embryo covers between two-thirds and three-quarters of the yolk circumference. The first reflective material is visible in the eyes.

Stage 39. *Three-quarters overgrowth (Figs. 4H, 10B′).* The embryo covers three-quarters of the yolk circumference. The dorsal portion of the eyes are now reflective and have a distinct gold color when viewed with a dissecting microscope. Melanocytes are present across almost the entire dorsal surface of the embryo. The pectoral fin buds begin to extend toward the posterior. The tail region begins to thin along the dorsal–ventral axis and the caudal fin begins to form. The lower jaw has formed but the jaw is not yet free to move.

Stage 40. *Full overgrowth (Figs. 5A, 10C′).* The embryo now extends around the entire circumference of the yolk. The caudal fin is growing in size and has a few rays. Melanocytes extend the entire length of the body, including onto the developing caudal fin. The gold coloration of the eyes now creates a gold ring around the lenses. The mid-gut has enlarged. Dark pigmentation is visible on the upper surface of the visceral cavity. The oral cavity is now open and the lower jaw is free to move.

Stage 41. *Early prehatching (Figs. 5B, 6B).* The tip of the tail extends over the head to the posterior of the eye. The iridocytes start to turn a brown-orange color. A few small round teeth are visible on the jaws. There are 30–32 cartilaginous vertebrae with neural and hemal arches forming. Ossification of the vertebrae and arches is under way. In the tail, the hypural plate cartilages are forming.

Stage 42. *Mid prehatching (Fig. 5C).* The tail extends over and to the side of the head and reaches the area of the pectoral fins. The iridocytes are now distinctly brown–orange. The dorsal and anal fin folds do not contain rays.

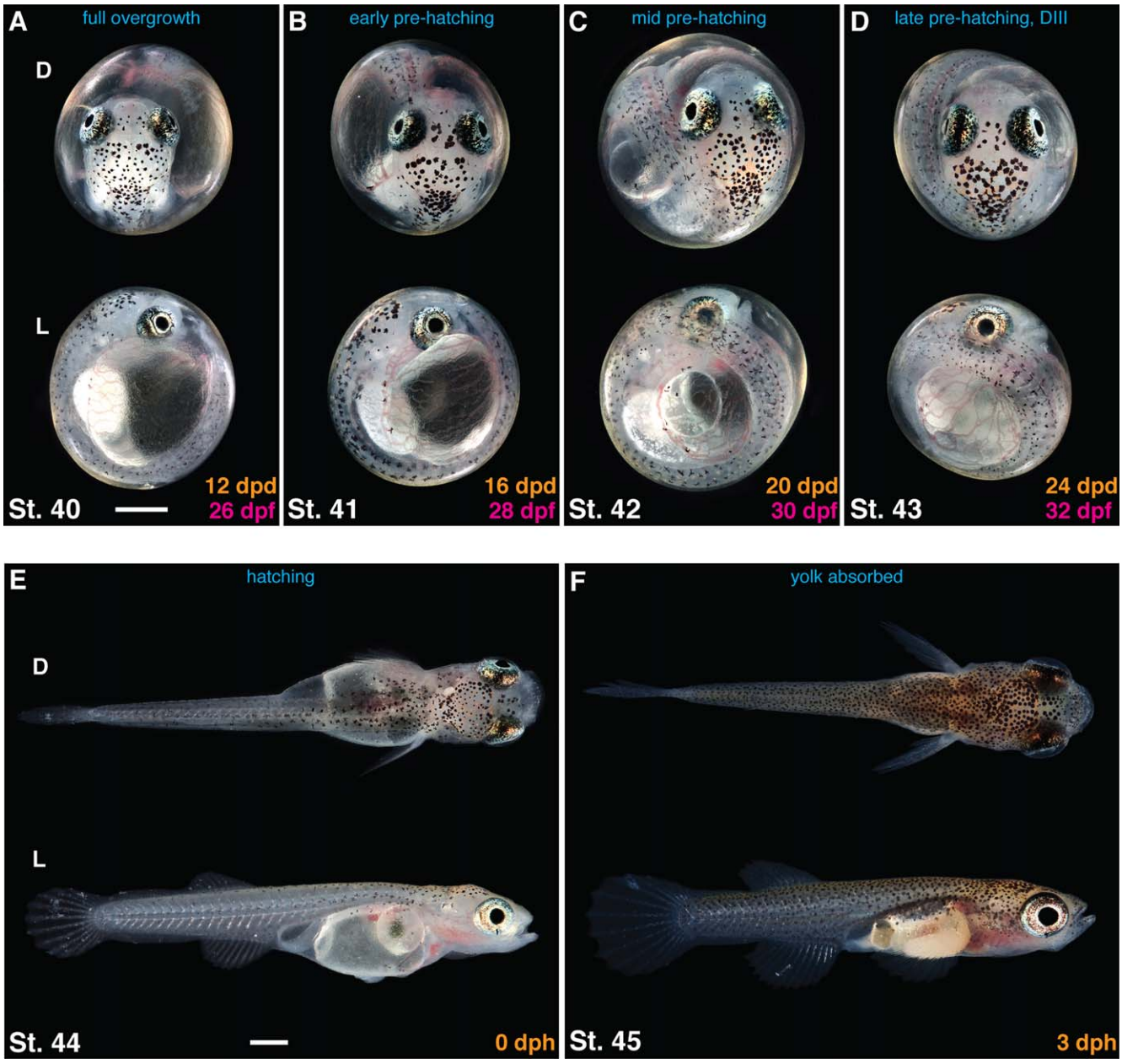

Fig. 5. **A–F:** Late development and hatching. Each panel contains a dorsal (D) and lateral (L) view of the embryo or larva. The timing of development at 25°C, in days postdiapause II (dpd) for embryos or days posthatch (dph) for larvae is provided in the lower right hand corner in orange for embryos on the diapause II trajectory, and in pink for embryos on the escape trajectory in days postfertilization (dpf). Note that these times are not exact, but should only be used as an approximation of when these stages typically occur. The scale bars in the lower portions of panels A and E indicate a length of 0.5 mm.

Stage 43. *Late prehatching, diapause III (Figs. 5D, 6C, 10D′).* There are many teeth on the lower jaw. Both the dorsal and anal fin folds contain rays, but are not pigmented by melanocytes. Pigmentation is absent on the pectoral fins as well. There are 30–32 ossified vertebrae and well-defined hypural plates in the caudal fin. Ossified rays are present in the pectoral and caudal fins, while cartilaginous rays are present in the anal and dorsal fins.

Stage 44. *Hatching (Fig. 5E).* The embryo has hatched, but is very similar in appearance and developmental state to Stage 43. The lipid droplet and some residual yolk are visible within the abdominal cavity which protrudes in both the lateral and ventral directions.

Stage 45. *Yolk absorbed (Fig. 5F).* The yolk has been mostly absorbed giving the fish a more streamlined appearance. The anal and dorsal fins are almost completely formed and the remaining fin fold tissues are largely regressed. Melanocytes and brown/orange iridocytes cover most of the dorsal surface giving the fish a darker appearance. Melanocytes are present on the dorsal, anal, and pectoral fins.

Stage 46. *Larva.* A week to 10 days later the anal and dorsal fin folds have completely regressed leaving the distinct dorsal and anal fins.

Adults. *(Fig. 7).* Adult females are torpedo shaped and mostly brown in color with a dark vertical bar running through the eye. Older females may eventually gain some blue-green coloration on the caudal fin and lower rear portion of the body. The anal fin width is much shorter than its length. Adult males have a deeper

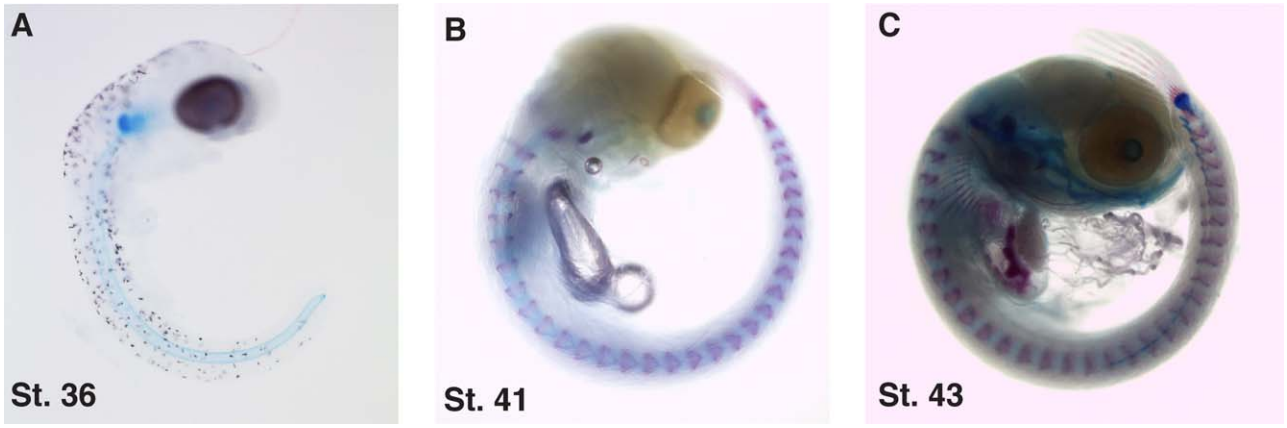

Fig. 6. **A–C:** Bone and cartilage staining. Alcian blue (cartilage) and alizarin red (bone) staining of postdiapause II embryos. Development of the axial skeleton begins at stage 36 and is not complete until after hatching. While the vertebrae begin to ossify before hatching, ossification of the cranial bones occurs during postembryonic development.

Fig. 7. Adult fish. Life-size images of adult *A. limnaeus*. Males are larger than females and have a distinctly deeper body profile, while females are smaller and more torpedo-shaped.

body with a distinct blue and blue-green tail. Young males tend to have lyre-shaped tails while older males often have paddle-shaped tails. There are numerous gold spots on the posterior half of the body. The anal fin is wider than it is long.

Differences in Development Between *A. limnaeus* and *A. myersi*

The development of *A. limnaeus* and *A. myersi* is very similar, but there are some subtle differences in timing, most of which have been observed during postdiapause II development. Perhaps the most substantial difference is in reference to the number of somite pairs. In *A. myersi*, Wourms described early postdiapause II embryos (Stage 34) as possessing 50 pairs of somites (Wourms, 1972a). In *A. limnaeus*,the total number of somite pairs appears to be 42, which is reached as the embryos enter into diapause II. Furthermore, escape embryos never seem to possess more than 42 pairs of somites. In fact, in early postdiapause II embryos (stages 34–36 and the equivalent escape stages E35a&tb), it is typically hard to count more than 38 pairs of somites, even in embryos that had 42 pairs when they entered diapause. This result has been interpreted as a differentiation of the most anterior somites into structures of the head which causes them to be obscured from view, or perhaps restructured. A more detailed analysis of somite differentiation is needed to better understand this aspect of development.

Another place where the two species differ is in the timing of gut formation and eye pigmentation during early postdiapause II development. In *A. myersi* pigmentation is absent in Stage 36 embryos, and first reported in Stage 37 embryos. In *A. limnaeus*, eye pigmentation is first visible at Stage 36. In addition, gut formation and the initiation of gut looping appears to begin earlier

in *A. limnaeus* compared with *A. myersi* as well (Stage 36 in *A.l.* vs. 38 in *A.m.*). The staging of these early embryos is partially based on the growth of the embryo in terms of length (how far around the yolk the body has grown). Because the embryos of the two species are approximately equal in size, this is likely not due to different sizes of the yolk mass. Perhaps the rate of trunk growth is slower in *A. limnaeus* than in *A. myersi* which results in apparent differences in the timing of other developmental characters.

Timing of Development

The median time it takes for embryos on the two developmental trajectories (those entering diapause II, and escape embryos that do not) to reach each developmental stage at 25°C is listed in the lower right hand corner of the staging images in Figures 1–5. These times are approximate based on many years of observation and should only be used as a rule of thumb. The rate and timing of development in *A. limnaeus* is apparently more variable than in many other species of fishes. This is likely due to: (1) the occurrence of dispersion and reaggregation, and (2) the interruption of development by diapause II. Developmental timing is reasonably synchronous until embryos complete epiboly and enter the dispersed cell phase (Stage 20). It appears that the timing of the reaggregation process is inherently variable, and thus the window of time for embryos to form an embryonic axis may vary by as much as 3 days, with the earliest embryos reaching the solid neural keel (Stage 28) at 9 days postfertilization (dpf), and the latest reaching it at 12 dpf. However, developmental rate from axis formation until entrance into diapause II appears to be similar in all embryos once the axis forms.

Under laboratory conditions embryos break diapause II spontaneously across a wide window of time (spanning months). In general, postdiapause II embryos develop at similar rates, but there is a degree of unexplained natural variation in postdiapause II developmental rate that may result in 3–4 days difference in time to reach Stage 43. This range of developmental rates is also observed in postdiapause II embryos that are forced to break diapause experimentally by exposure to 48 hr of constant light at 30°C. For escape embryos, there is a definite range of developmental rates with some embryos developing significantly faster than others and clearly reaching stage E31 after 15 dpf while others do not reach this morphology until approximately 20 dpf. This initial difference in rate appears to be sustained though the entirety of development.

Developmental rate and timing does not appear to be female-specific, as a single clutch of embryos may contain embryos that develop across the entire range of variation described above. Wourms referred to this type of variation within a single clutch of eggs as the "multiplier effect" and explained this in terms of variation in the occurrence and duration of each diapause stage leading to many different developmental pathways (Wourms, 1972c). These different pathways are theorized to have different chances of survival under different sets of environmental conditions. The variation in developmental rate and timing reported here may be another mechanism to increase variation and thus spread risk across a range of phenotypes. It is possible that this variation is natural and adaptive and ensures that not all the embryos receive the same environmental cues during any particular "critical" window in development when phenotype may be altered, and thus ensuring a wide range of developmental phenotypes. Alternatively, this variation could be the product of incubation under laboratory conditions with the absence of normal environmental cues. Observation of embryos under natural conditions are needed to better explain the potential importance of this variation in developmental timing.

Development is slow in *A. limnaeus* compared with other non-annual killifishes with similar sized embryos such as *Kryptolebias marmoratus* or *Fundulus heteroclitus* (DiMichele and Powers, 1982; Mourabit et al., 2011). In the 12–14 days that it takes for these two species to reach hatching competence, *A. limnaeus* is only just developing the solid neural keel. For escape embryos of *A. limnaeus*, the late prehatching stage (Stage 43) is not reached until approximately 32 days postfertilization. Even if the approximately 8 days the embryos spend in the dispersion and reaggregation phases of development (unique to annual killifishes) are taken into account, the overall developmental rate is roughly half that of other cyprinodont fishes with similar sized embryos incubated at similar temperatures.

Maternal to Zygotic Transition

In all vertebrates, the earliest developmental stages are controlled by maternally packaged transcripts and the zygotic genome is thought to be largely transcriptionally inactive (Baroux et al., 2008; Tadros and Lipshitz, 2009). In zebrafish and other fishes, zygotic genome activation is thought to occur at the mid-blastula transition (Kane and Kimmel, 1993). In *A. limnaeus*, inhibition of embryos with actinomycin-D, an inhibitor of transcription, just after fertilization causes embryos to stall in development at Stage 12, the early flat hollow blastula (Fig. 1L). Without the ability to support transcription of the zygotic genome, embryos stall in this stage and then either die or begin to show signs of abnormal development (Fig. 8). Of interest, continued expansion of the blastoderm and migration of the deep blastomeres is completely blocked and most of them appear to die. Furthermore, the ENVL cells are no longer able to continue flattening and begin to looked "rounded." These patterns suggest that the zygotic genome is likely activated just before the stages of development that require cell movements associated with epiboly, but after the initial differentiation of deep cells from the enveloping cell layer cells.

Dispersion and Reaggregation Stages

The dispersion and reaggregation stages (Fig. 3) are unique to annual killifish, but there is a great deal of variation among species in the number and size of cells that participate in reaggregation (Wourms, 1972b). In *A. limnaeus* over 8,000 deep blastomeres are present during reaggregation (Fig. 9), with only approximately 25% of those participating in the formation of the early aggregate (Cleaver, 2012). These stages are difficult to follow using standard light microscopy, and thus cell staining techniques are helpful in observing cells during these stages.

The "Escape" and Diapause II Trajectories

Entrance into diapause II is an alternative developmental trajectory in annual killifishes that includes different timing in the development of anterior structures compared with the posterior structures (Podrabsky et al., 2010; Furness et al., 2015). Thus, strictly counting somites does not work for staging embryos on the two different trajectories. While there are several stages that are unique to each trajectory, once the embryos reach Stage 36,

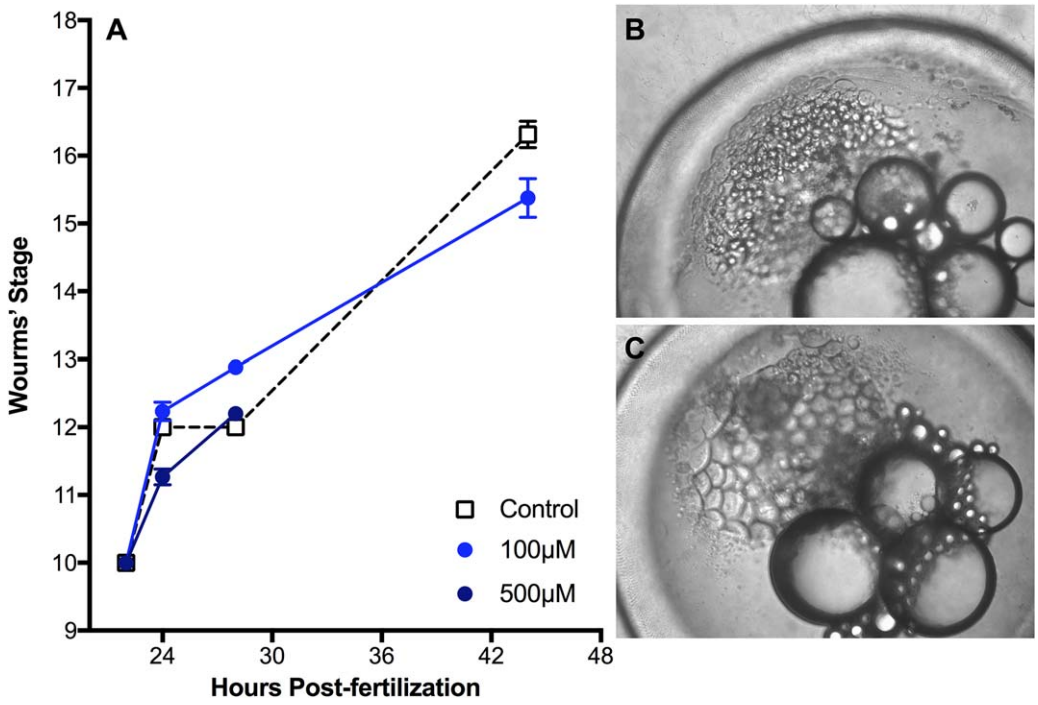

Fig. 8. Mid-blastula transition. **A:** Incubation in actinomycin-D to block transcription stalls embryo development at Stage 12, the early hollow blastula stage. **B,C:** A normal Stage 12 embryo (B) at 24 hr postfertilization (hpf), and an abnormal embryo (C) at 44 hpf illustrating the loss of deep blastomeres and the lack of embryo expansion.

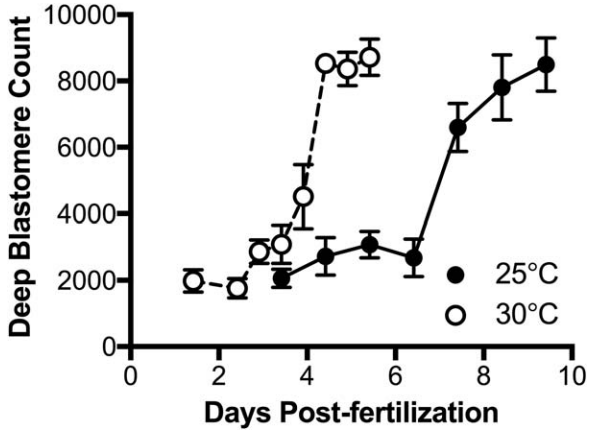

Fig. 9. Number of cells present during dispersion and reaggregation. There are over 8,000 cells present in the embryo when the aggregate begins to form. Temperature does not alter the number of cells present at the time of reaggregation, but it does appear to alter the timing of cell proliferation and aggregate formation.

they are roughly equivalent as judged by gross morphology. It is entirely possible, and perhaps even probable that there are differences in the timing of organ system development and physiology in escape and diapause trajectory embryos. However, at this time we do not have the detailed data needed to separate the trajectories from Stage 36 to 43, and thus those stages are used for both trajectories.

Emerging Model Organisms

The usefulness of traditional model organisms is undeniable. Work over the past several decades on these species has produced volumes of literature and commercially available resources that can relatively easily be applied to developmental studies. This work has been instrumental in creating a model that generalizes developmental processes. However, it is important as scientists, mentors, and classroom instructors, that we identify these generalized models for what they are—a conceptual framework for describing and explaining the developmental process. It is clear that not all organisms develop using the exact same mechanisms or processes, and for the past several decades we have not, as a collective, wholly embraced the incredible diversity of developmental patterns, processes, and capabilities that exist in nature.

If we are to truly understand development, and how it is linked to ecological and evolutionary processes, we must look beyond the current handful of model organisms. It is now possible to generate the necessary molecular and genetic resources and tools needed to study the mechanisms of development in almost any organism. Thus, it is time that we focus our efforts on using the diversity that nature has offered to strengthen our understandings of the basic processes that unify, as well as the unique and specific processes that contribute to the enormous biodiversity that we observe. Studies of development in the annual killifish, *A. limnaeus* can not only lend insights into fundamental processes in development, but also allows for exploring questions that simply cannot be addressed in other models, because those other species have not evolved the unique suite of traits present in these fish.

Experimental Procedures

Husbandry and Collection of Embryos

Adult *Austrofundulus limnaeus* were originally collected near the town of Quisiro, Estado Zulia, in the Maracaibo Basin of

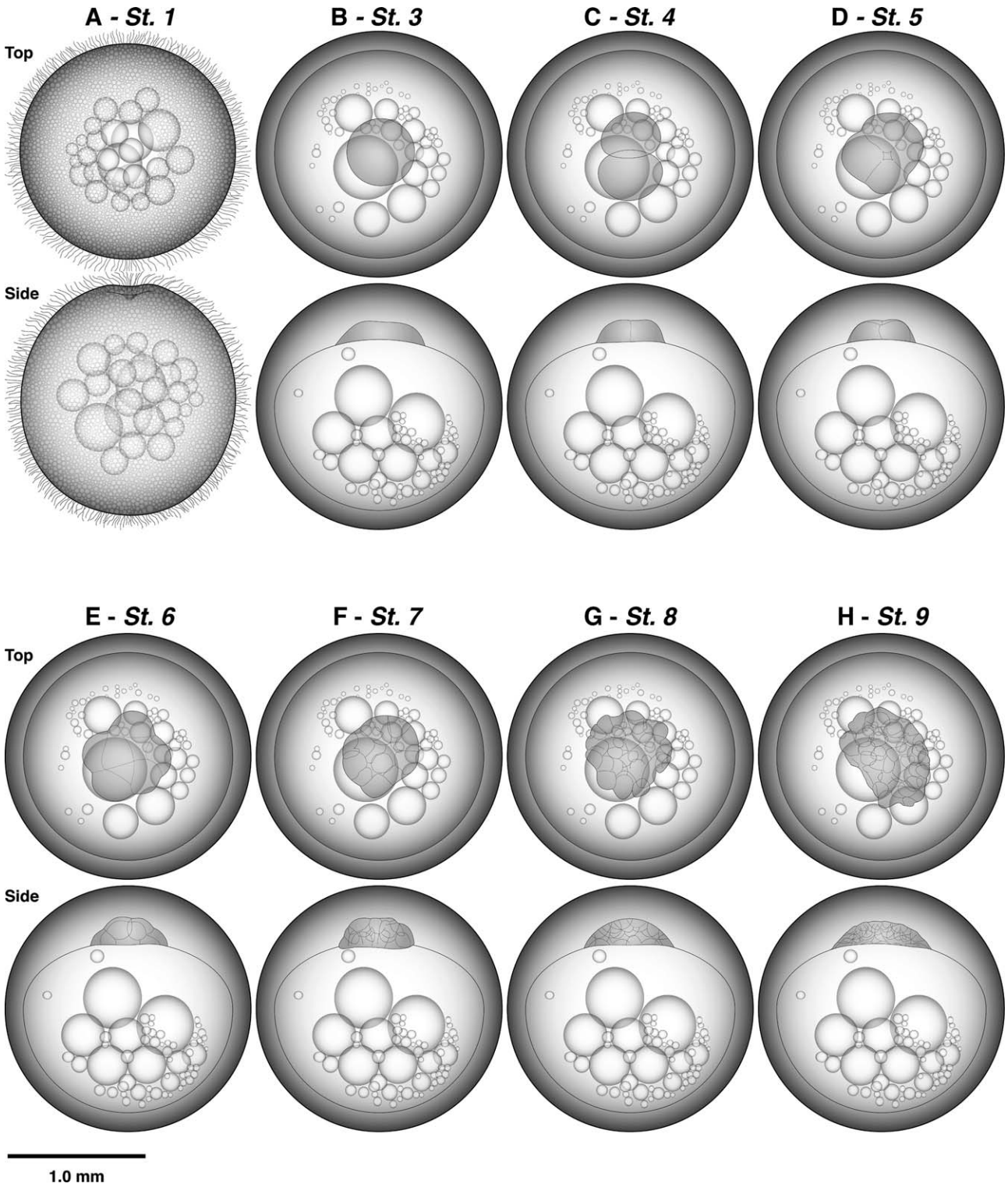

Fig. 10. Line drawings of key stages in the development of *A. limnaeus*. Illustrations were created in Adobe Illustrator based on photographs of embryos. Illustrations are especially useful for side views of embryos between stages 28 and 34, where live images are difficult to capture due to the yolk obscuring the view. The last panel of the figure is a key to the anatomy of embryos.

Venezuela in 1995 (Podrabsky et al., 1998). Fish were housed and cared for at Portland State University according to previously described methods (Podrabsky, 1999) as approved by PSU IACUC protocols (PSU protocols #16 & 33). Embryos were collected using natural spawning activity by placing a tray of 0.5 mm glass beads into a tank with a single pair of fish. Collected embryos were kept at 25°C in the dark in a temperature controlled incubator when not under observation. To create a synchronized cohort of postdiapause II embryos, diapause was broken by exposing the embryos to constant light at 30°C for 48 hr.

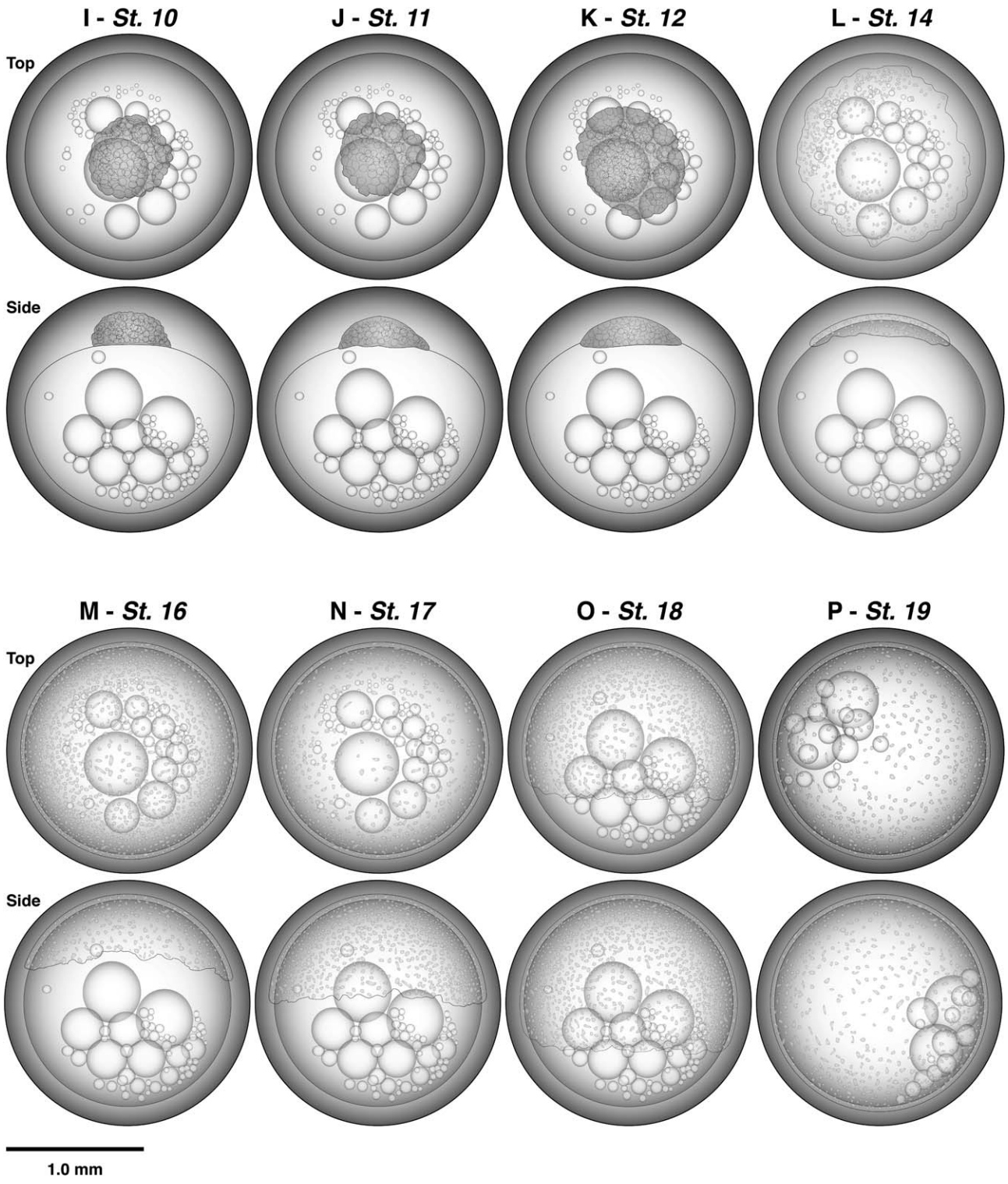

Fig. 10. Continued.

Microscopic Observation and Imaging of Whole Embryos

To improve the visibility of embryonic structures in live embryos, the chorionic hairs were mechanically removed by rolling the embryos with an index finger on a moist KimWipe for 20–30 sec or until the chorion was smooth and devoid of hairs.

Embryos were prepared for imaging by placing them in a 1.5-mm-deep well depression slide and covering them with a coverslip. Excess embryo medium was blotted from under the coverslip by wicking it away with a KimWipe. This procedure allowed the embryo to be rotated and positioned by moving the coverslip in relation to the slide. The embryos were then placed over a black

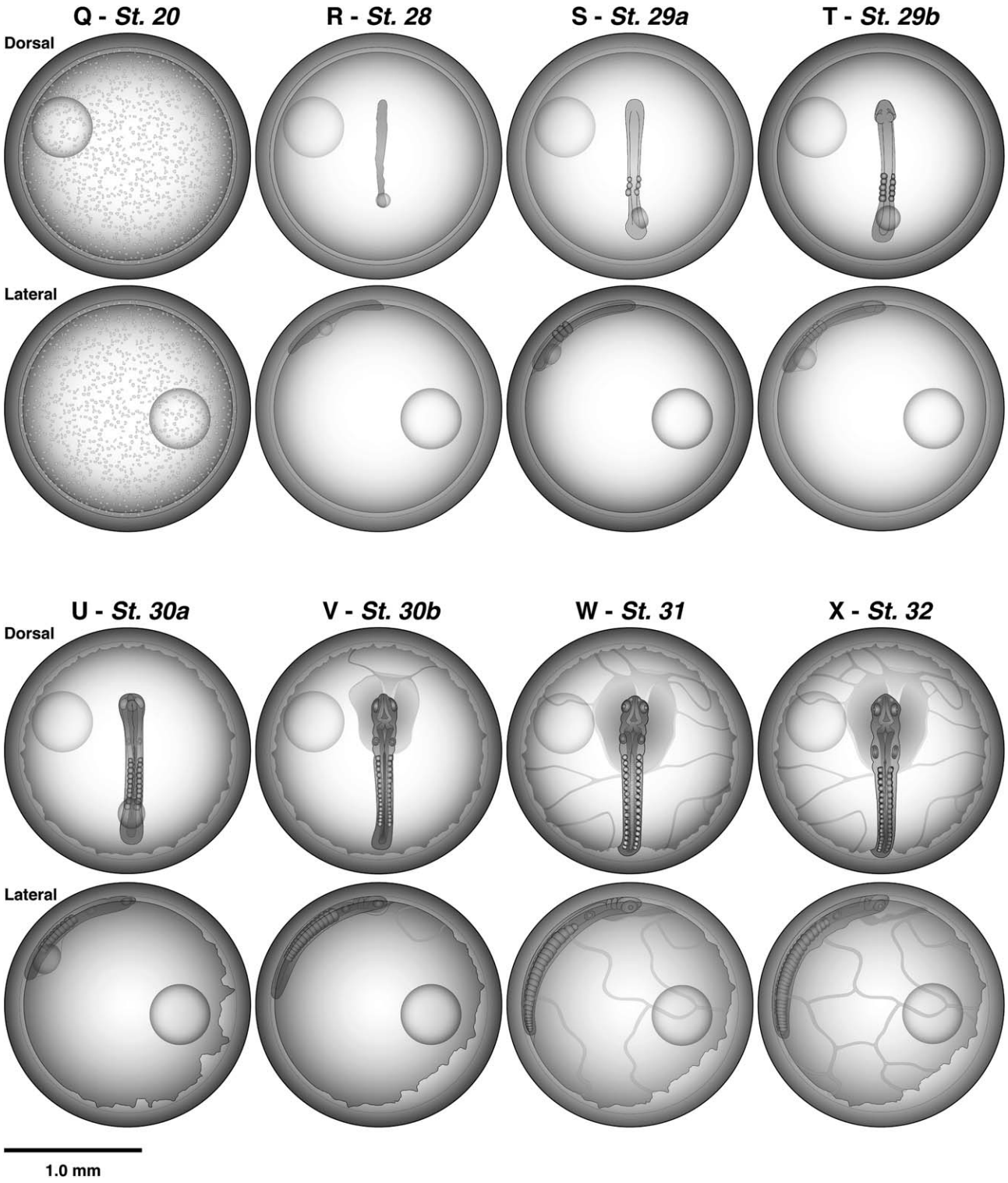

Fig. 10. Continued.

background and images were captured using the Big Kahuna macro digital imaging system (Dun, Inc., Virginia, USA) in the California Academy of Sciences Project lab. Multiple images were taken and extended depth of field was generated by image stacking. Minor alterations to the brightness and contrast of images was used to achieve optimal exposure and contrast.

Imaging of Dispersion and Reaggregation Phases

Embryos were fixed with BT fixative solution consisting of 4% paraformaldehyde, 0.15 M $CaCl_2$, 4% sucrose in 0.1 M $NaPO_4$, pH 7.4 (Westerfield, 1995) at 4°C for 48 hr. The chorion of each embryo was pierced with an insect pin to allow a more rapid infusion of the fixative. Following fixation, the embryos were

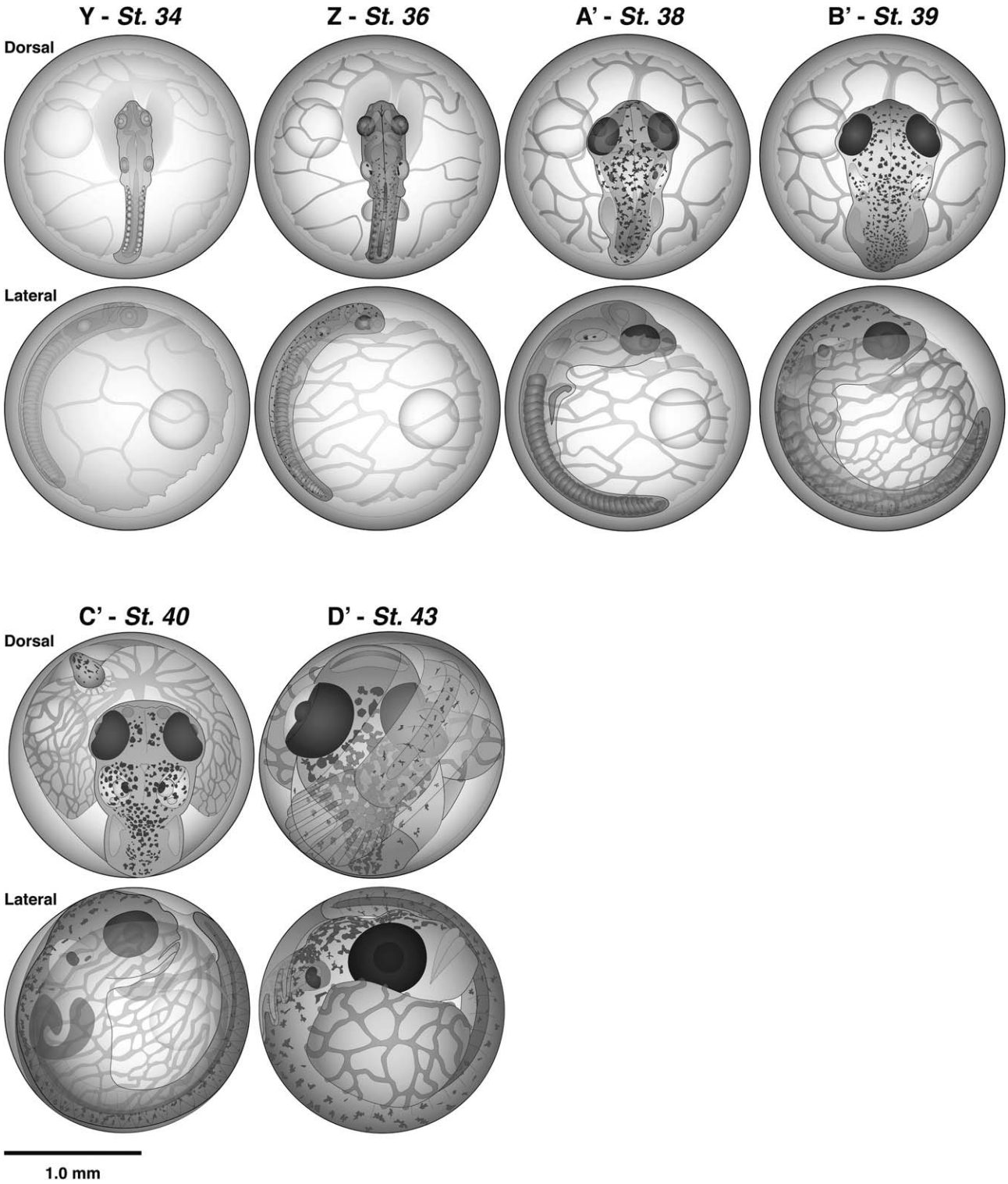

Fig. 10. Continued.

dechorionated with fine tip forceps, and dehydrated by a series of 5 min washes in 50%, 70%, 95%, and 100% methanol. Embryos were washed twice and then stored in 100% methanol at -20°C. Embryos were permeabilized in phosphate buffered saline (PBS) with 0.5% Tween-20 for 24 hr at room temperature, and then washed for 5 min in PBS. Embryos were incubated for 5 min at room temperate with 10 μg/ml Hoechst 33258 in PBS. Staining was followed by a 5-min wash in PBS.

The embryos were then soaked in SlowFade Gold antifade (Invitrogen) for at least 45 min before being cubed in agarose. Each side of the "cubed" embryos was imaged using a Leica DMIRB inverted compound microscope equipped with

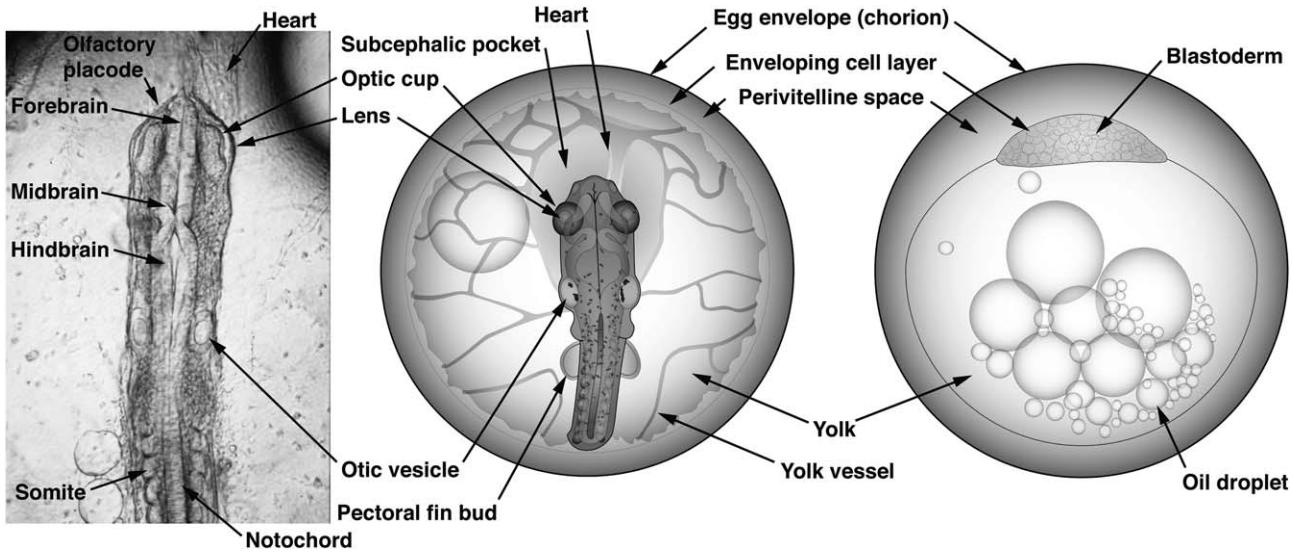

Fig. 10. Continued.

epifluorescence. For each of the six sides of the cube, a stack of 11 focal planes (taken every 20 microns) at 100× magnification were captured to create a single composite image. For counting the number of cells, images were digitally processed using the maximum intensity composite algorithm in ImagePro Plus (Media Cybernetics, Bethesda, MD). The images were then cropped, converted to grayscale, color inverted, and flattened using the Flatten Image function. The gamma was adjusted to 46 from 50 and the contrast to 61 from the original value of 50.

Inhibition of Development with Actinomycin-D

The embryos were soaked in embryo medium containing 0, 100, and 500 μM actinomycin-D (Sigma-Aldrich, St. Louis, MO) prepared from a stock solution in dimethyl sulfoxide (DMSO). The final concentration of DMSO was 1%, and this amount of DMSO was added to the control embryos as well. Medium was changed every 24 hr. Embryos were inspected and staged at 0, 22, 24, 28, and 44 hours postfertilization (hpf). Representative images were captured using a Leica digital camera mounted to the microscope.

Bone and Cartilage Staining

Bone and cartilage staining methods were modified from existing protocols (Walker and Kimmel, 2007). Embryos were fixed for 2 hr at room temperature (RT) in 2% paraformaldehyde in PBS. The embryos were washed for 20 min in 100 mM Tris, 20 mM $MgCl_2$, pH 7.5 before overnight staining in 0.04% alcian blue in 20 mM $MgCl_2$ at RT. Embryos were washed for 15 min each in 80, 50, and 25% ethanol diluted in the Tris-$MgCl_2$ buffer. A mixture of 3% hydrogen peroxide and 0.5% KOH was used to bleach the embryos for 20 min at RT, followed by 2 × 40 min washes in 25% glycerol, 0.1% KOH. Embryos were stained in 0.01% alizarin red, pH 7.5 for 1 hr at RT, followed by destaining in multiple washes of 50% glycerol, 0.1% KOH until tissues were clear of stain. Embryos were stored in 100% glycerol.

Acknowledgments

We thank the California Academy of Sciences for allowing us to use their "Big Kahuna" camera to capture the images presented here, and for all the visitors to the academy that watched us working in the project lab and asked great questions about our work. We would also like to thank Kylie J. Brown for creating the illustrations of some key developmental stages presented in Figure 10. J.E.P. was supported by a National Science Foundation award.

References

Baroux C, Autran D, Gillmor C, Grimanelli D, Grossniklaus U. 2008. The maternal to zygotic transition in animals and plants. Cold Spring Harb Symp Quant Biol 73:89–100.

Cleaver T. 2012. The effects of temperature on the dispersion and reaggregation stages of development in the annual killifish, Austrofundulus limnaeus. In: Biology. Portland, OR: Portland State University.

Dahl G. 1958. Two new annual cyprinodont fishes from northern Colombia. Stanford Ichthyol Bull 7:42–46.

DiMichele L, Powers DA. 1982. LDH-B genotype-specific hatching times of Fundulus heteroclitus embryos. Nature 296:563–564.

Furness AI. 2016. The evolution of an annual life cycle in killifish: adaptation to ephemeral aquatic environments through embryonic diapause. Biol Rev 91:796–812.

Furness AI, Reznick DN, Springer MS, Meredith RW. 2015. Convergent evolution of alternative developmental trajectories associated with diapause in African and South American killifish. Proc Biol Sci 282: pii 20142189.

Genade T, Benedetti M, Terzibasi E, Roncaglia P, Valenzano DR, Cattaneo A, Cellerino A. 2005. Annual fishes of the genus Nothobranchius as a model system for aging research. Aging Cell 4: 223–233.

Kane DA, Kimmel CB. 1993. The zebrafish midblastula transition. Development 119:447–456.

Mourabit S, Edenbrow M, Croft DP, Kudoh T. 2011. Embryonic development of the self-fertilizing Mangrove Killifish Kryptolebias marmoratus. Dev Dyn 240:1694–1704.

Podrabsky J, Riggs C, Wagner J. 2016. Tolerance of Environmental Stress. In: Berois N, García G, De Sá R, editors. Annual fishes. Life history strategy, diversity, and evolution. Boca Raton, FL: CRC Press, Taylor & Francis. p 159–184.

Podrabsky JE. 1999. Husbandry of the annual killifish Austrofundulus limnaeus with special emphasis on the collection and rearing of embryos. Environ Biol Fish 54:421–431.
Podrabsky JE, Garrett IDF, Kohl ZF. 2010. Alternative developmental pathways associated with diapause regulated by temperature and maternal influences in embryos of the annual killifish Austrofundulus limnaeus. J Exp Biol 213:3280–3288.
Podrabsky JE, Hrbek T, Hand SC. 1998. Physical and chemical characteristics of ephemeral pond habitats in the Maracaibo basin and Llanos region of Venezuela. Hydrobiologia 362:67–78.
Polačik M, Podrabsky JE. 2015. Temporary environments. In: Riesch R, Tobler M, Plath M, editors. Extremophile fishes: ecology, evolution, and physiology of teleosts in extreme environments. Cham, Switzerland: Springer. p 217–245.
Romney A, Podrabsky J. 2017. Transcriptomic analysis of maternally provisioned cues for phenotypic plasticity in the annual killifish, Austrofundulus limnaeus. Evodevo 8:6.
Romney A, Riggs C, Podrabsky J. 2015. Bioproject PRJNA272154. Transcriptome analysis in Austrofundulus limnaeus embryos. Available at: http://www.ncbi.nlm.nih.gov/bioproject/272154.
Schultz L. 1949. A further contribution to the ichthyology of Venezuela. Proc U S Natl Mus 99:79–211.
Tadros W, Lipshitz HD. 2009. The maternal-to-zygotic transition: a play in two acts. Development 136:3033–3042.
Wagner J, Warren W, Minx P, Podrabsky J. 2015. Austrofundulus limnaeus 1.0 draft genome assembly with annotation. Bethesda, MD: National Center for Biotechnology Information.
Wagner JT, Podrabsky JE. 2015. Extreme tolerance and developmental buffering of UV-C induced DNA damage in embryos of the annual killifish Austrofundulus limnaeus. J Exp Zool 323A:10–30.
Walker M, Kimmel C. 2007. A two-color acid-free cartilage and bone stain for zebrafish larvae. Biotech Histochem 82:23–28.
Westerfield M. 1995. The zebrafish book: a guide for the laboratory use of zebrafish (Brachydanio rerio). Eugene, OR: M. Westerfield.
Wourms JP. 1972a. The developmental biology of annual fishes I. Stages in the normal development of Austrofundulus myersi Dahl. J Exp Zool 182:143–168.
Wourms JP. 1972b. The developmental biology of annual fishes II. Naturally occurring dispersion and reaggregation of blastomeres during the development of annual fish eggs. J Exp Zool 182: 169–200.
Wourms JP. 1972c. The developmental biology of annual fishes III. Pre-embryonic and embryonic diapause of variable duration in the eggs of annual fishes. J Exp Zool 182:389–414.